

1 **Validation and application of optimal ionospheric shell height model**
2 **for single-site TEC estimation**

3 Jiaqi Zhao¹, Chen Zhou¹

4 School of Electronic Information, Wuhan University, Wuhan, 430072, China

5 Corresponding to: chenzhou@whu.edu.cn

6

7 **Abstract**

8 We recently proposed a method to establish optimal ionospheric shell height model
9 based on the international GNSS service (IGS) station data and the differential code
10 bias (DCB) provided by Center for Orbit Determination in Europe (CODE) during the
11 time from 2003 to 2013. This method is very promising for DCB and accurate total
12 electron content (TEC) estimation by comparing to traditional fixed shell height
13 method. However, this method is basically feasible only for IGS stations. In this study,
14 we investigate how to apply the optimal ionospheric shell height derived from IGS
15 station to non-IGS stations or isolated GNSS receivers. The intuitional and practical
16 method to estimate TEC of non-IGS stations is based on optimal ionospheric shell
17 height derived from nearby IGS stations. To validate this method, we selected two
18 dense networks of IGS stations located in US and Europe region. Two optimal
19 ionospheric shell height models are established by two reference stations, namely
20 GOLD and PTBB, which are located at the approximate center of two selected
21 regions. The predicted daily optimal ionospheric shell heights by the two models are

22 applied to other IGS stations around these two reference stations. Daily DCBs are
23 calculated according to these two optimal shell heights and compared to respective
24 DCBs released by CODE. The validation results of this method present that 1)
25 Optimal ionospheric shell height calculated by IGS stations can be applied to its
26 nearby non-IGS stations or isolated GNSS receivers for accurate TEC estimation. 2)
27 As the distance away from the reference IGS station becomes larger, the DCB
28 estimation error becomes larger. The relation between the DCB estimation error and
29 the distance is generally linear.

30

31 **Keyword**

32 Ionospheric shell height, Single layer model (SLM), Differential code bias (DCB),
33 Total electron content (TEC)

34

35 **Introduction**

36 Dual-frequency GPS signals propagation are affected effectively by ionospheric
37 dispersive characteristic. While, by taking advantage of this property, ionospheric
38 TEC along the path of signal can be estimated by using differencing the pseudorange
39 or carrier phase observations from dual-frequency GPS signals. Carrier phase
40 leveling/smoothing of code measurement is widely adopted to improve the precision
41 of absolute TEC observations (Mannucci et al., 1998; Horvath and Crozier, 2007). In

42 general, it is considered that the derived TEC in carrier phase leveling/smoothing
43 technique consists of slant TEC (STEC), the combination differential code bias (DCB)
44 of satellite and receiver, multipath effects and noise. The DCB is usually considered
45 as the main error source and could be as large as several TECu (Lanyi and Roth, 1988;
46 Warnant 1997).

47 For TEC and DCB estimations, mapping function with single layer model (SLM)
48 assumption have been intensively studied for many years. Sovers and Fanelow (1987)
49 firstly simplified the ionosphere to a spherical shell. They set the bottom and the top
50 side of the ionospheric shell as $h-35$ and $h+75$ km, where h is taken to be 350 km
51 above the surface of the earth and allowed to be adjusted. In this model, the electron
52 density was evenly distributed in the vertical direction. Based on this model, Sardón et
53 al. (1994) introduced the Kalman filter method for real-time ionospheric VTEC
54 estimation, which can also be promising prediction of DCBs under adverse conditions
55 (antispoofing, ionospheric disturbances). Klobuchar (1987) assumed that STEC
56 equals VTEC multiplied by the approximation of the standard geometric mapping
57 function at the mean vertical height of 350 km along the path of STEC. Lanyi and
58 Roth (1988) further developed this model into a single thin-layer model, and proposed
59 the standard geometric mapping function and the polynomial model. The single
60 thin-layer model assumed that the ionosphere is simplified by a spherical thin shell
61 with infinitesimal thickness. Clyne et al (1989) proposed a mapping function in the
62 form of a polynomial by assuming a homogeneous electron density shell between

63 altitudes of 200 and 600 km. Mannucci et al (1998) presented an elevation scaling
64 mapping function derived from extended slab mode. There are also many modified
65 mapping function according to the standard geometric mapping function. Schaer
66 (1999) proposed the modified standard mapping function using a reduced zenith angle.
67 Rideout and Coster (2006) presented a new mapping function which replaces the
68 influence of the shell height by an adjustment parameter, and set the shell height as
69 450 km. Smith et al (2008) modified the standard mapping function by using a
70 complex factor. Based on the electron density field derived from the international
71 reference ionosphere (IRI), Zus et al (2017) recently developed an ionospheric
72 mapping function at fixed height of 450 km with dependence on time, location,
73 azimuth angle, elevation angle, and different frequencies.

74 Ionospheric shell height is considered to be the most important parameter for
75 mapping function, and the shell height is typically set to a fixed value between 350
76 and 450 km (Lanyi and Roth, 1988; Mannucci et al., 1998). Birch et al. (2002)
77 proposed an inverse method for estimate the shell height by using simultaneous
78 VTEC and STEC observations, and suggested the shell height is preferred to be a
79 value between 600 and 1200 km. Nava et al. (2007) utilized multiple stations to obtain
80 a shell height estimation method by minimizing the mapping function errors, this
81 method is referred as the “coinciding pierce point” technique. Their results indicated
82 that the suitable shell heights for the mid-latitude is 400 km and 500 km during the
83 geomagnetic undisturbed conditions and disturbed conditions, respectively. In the

84 case of the low-latitude, the shell height at about 400 km is suitable for both quiet and
85 disturbed geomagnetic conditions. Jiang et al. (2018) applied this technique to
86 estimate the optimal shell height for different latitude bands. In their case, the optimal
87 layer height is about 350 km for the entire globe. Brunini et al. (2011) studied the
88 influence of the shell height by using an empirical model of the ionosphere, and
89 pointed out that a unique shell height for whole region does not exist. Li et al. (2018)
90 applied a new determination method of the shell height based on the combined IGS
91 GIMs and the two methods mentioned above to the Chinese region, and indicated that
92 the optimal shell height in China ranges from 450 to 550 km. Wang et al. (2016)
93 studied the shell height for grid-based algorithm by analyzing goodness of fit for
94 STEC. Lu et al. (2017) applied this method to different VTEC models, and
95 investigated the optimal shell heights at solar maximum and at solar minimum.

96 In the recent study by Zhao and Zhou (2018), a method to establish optimal
97 ionospheric shell height model for single station VTEC estimation has been proposed.
98 This method calculates the optimal ionospheric shell height with regards to minimize
99 $|\Delta\text{DCB}|$ by comparing to the DCB released by CODE. Five optimal ionospheric shell
100 height models were established by the proposed method based on the data of five IGS
101 stations at different latitudes and the corresponding DCBs provided by CODE during
102 the time 2003 to 2013. For the five selected IGS stations, the results have shown that
103 the optimal ionospheric shell height models improve the accuracies of DCB and TEC
104 estimation comparing to fixed ionospheric shell height of 400 km in a statistical sense.

105 We also found that the optimal ionospheric shell height show 11-year and 1-year
106 periods and is related to the solar activity, which indicated the connection of the
107 optimal shell height with ionospheric physics.

108 While the proposed optimal ionospheric shell height model is promising for
109 DCB and TEC estimation, this method also can be implemented to isolated GNSS
110 receivers not belonging to IGS stations, if we can get the long-term observations and
111 reference values of DCB from the isolated GNSS receivers. The purpose of this study
112 is to investigate the application of the optimal ionospheric shell height derived from
113 IGS station to non-IGS stations. By considering the spatial correlation of ionospheric
114 electron density, it is intuitive and practical to adopt the optimal ionospheric shell
115 height of a nearby IGS station for the non-IGS stations.

116 The purpose of this study is to investigate the feasibility of applying the optimal
117 ionospheric shell height derived from IGS station to nearby non-IGS GNSS receivers
118 for accurate TEC/DCB estimation. By selecting two different regions in U.S. and
119 Europe with dense IGS stations, we calculate the daily DCBs of 2014 by using the
120 optimal ionospheric shell heights derived from 2003-2013 data of two central stations
121 in two regions. We also try to find the DCB estimation error and its relation to
122 distance away from the central reference station.

123

124 **Method**

125 In (Zhao and Zhou, 2018), we proposed a concept of optimal ionospheric shell height
 126 for accurate TEC and DCB estimation. Based on daily data of single site, this
 127 approach searches daily optimal ionospheric shell height, which minimizes the
 128 difference between the DCBs calculated by VTEC model for single site and reference
 129 values of DCB. For a single site, its long-term daily optimal ionospheric shell heights
 130 can be estimated and then modeled. In our case, the polynomial model (Wild, 1994;
 131 Komjathy, 1997) is applied to estimate satellite and receiver DCBs, and the DCBs
 132 provided by CODE are used as the reference.

133 In the polynomial model, the VTEC is considered as a Taylor series expansion in
 134 latitude and solar hour angle, which is expressed as follows:

$$135 \quad T_v(\varphi, S) = \sum_{i=0}^m \sum_{j=0}^n E_{ij} (\varphi - \varphi_0)^i (S - S_0)^j \quad (1)$$

136 where T_v denotes VTEC. φ and S denote the geographic latitude and the solar
 137 hour angle of ionospheric pierce point (IPP), respectively; φ_0 and S_0 denote φ
 138 and S at regional center. E_{ij} is the model coefficient. m and n denote the
 139 orders of the model. A polynomial model fits the VTEC over a period of time. In our
 140 case, a VTEC model is generated over 3 hours of time, therefore 8 VTEC models are
 141 applied per day. DCB is considered as constant in one day. Since our analysis is based
 142 on long-term single site data, we set m and n to 4 and 3, respectively. Huang and
 143 Yuan (2014) applied the polynomial model with the same orders to TEC estimation.

144 Based on the thin shell approximation, the observation equation can be written
 145 as:

$$146 \quad T_{os}^{PRN}(\varphi, S) = T_v(\varphi, S) \cdot f(z) + DCB^{PRN} \quad (2)$$

147 where T_{os}^{PRN} is slant TEC calculated by carrier phase smoothing, the superscript PRN
 148 denotes GPS satellite. DCB^{PRN} denotes the combination of GPS satellite and
 149 receiver DCB. z denotes the zenith angle of IPP. According to Lanyi and Roth (1988),
 150 the standard geometric mapping function $f(z)$ is expressed as follows:

$$151 \quad f(z) = 1/\cos(z) \quad (3)$$

$$152 \quad z = \arcsin \frac{Re \cdot \cos El}{Re + h} \quad (4)$$

153 where Re denotes the earth's radius, El denotes the elevation angle, and h denotes
 154 the thin ionospheric shell height. Note that h also affects the location of IPP.

155 To estimate DCBs, The method above requires a definite thin shell height value.
 156 Conversely, if we get the daily solutions of DCBs, the optimal ionospheric shell
 157 height can be estimated. The optimal ionospheric shell height is assumed to be
 158 between 100 and 1000 km and is defined as the shell height with the minimum
 159 difference between DCB^{PRN} and the reference values. This optimization problem can
 160 be written as:

$$161 \quad \min_{100 < h < 1000} \text{mean}(|\mathbf{DCB}_{\text{ref}} - \mathbf{DCB}|) \text{ s.t. } \mathbf{T} = \mathbf{\Phi} \cdot \mathbf{E} + \mathbf{\theta} \cdot \mathbf{DCB} \quad (5)$$

162 where h is the daily optimal ionospheric shell height, $\mathbf{DCB}_{\text{ref}}$ denotes the vector of
 163 the reference values of DCBs, s.t. is the abbreviation for subject to,
 164 $\mathbf{T} = \mathbf{\Phi} \cdot \mathbf{E} + \mathbf{\theta} \cdot \mathbf{DCB}$ is the matrix form of all the observation equations in one day,
 165 \mathbf{T} denotes the vector of T_{os} , \mathbf{E} corresponds to the coefficients of the models,
 166 \mathbf{DCB} is the vector of DCB^{PRN} , $\mathbf{\Phi}$ and $\mathbf{\theta}$ are the coefficient matrix of \mathbf{E} and
 167 \mathbf{DCB} , respectively.

168 After the method above is applied to 11-year data, the estimated optimal
169 ionospheric shell heights can be modeled by a Fourier series, which is expressed as
170 follows:

$$171 \quad h(x) = a_0 + \sum_{n=1}^k \left(a_n \cos \frac{2n\pi x}{L} + b_n \sin \frac{2n\pi x}{L} \right) \quad (6)$$

172 where k is the order of Fourier series and is set to 40, a_n and b_n are the model
173 coefficients, x is the time, and L is the time span which equals to 4018 days. The
174 maximum frequency of model is $40/L \approx 0.01$ per day, which corresponds to a period
175 of 100 days. By least square method, the model coefficients can be estimated.

176 This model can be applied to neighboring stations' DCB estimation. Instead of
177 fixed shell height, this model provide predicted optimal ionospheric shell height.
178 While in the establishment and application of the model, the VTEC model, mapping
179 function and elevation cut-off angle can't change. Both of them affect the optimal
180 ionospheric shell height.

181

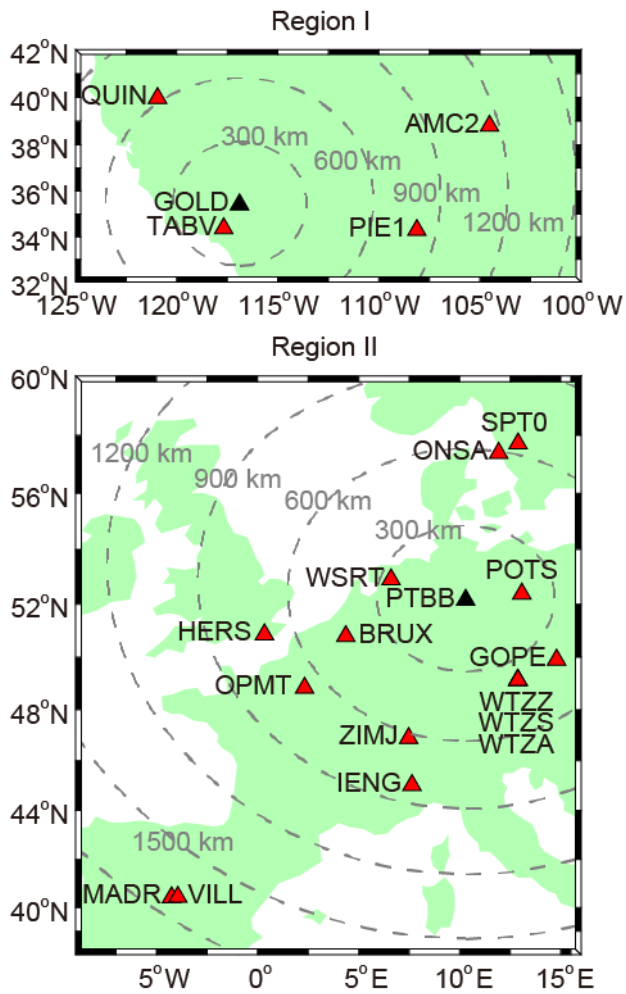
182 **Experiment and Results**

183 The previous section introduced a method to establish daily optimal ionospheric shell
184 height model based on single site with reference values of DCBs. To analyze the
185 improvement of DCB estimation by this model for the reference station and other
186 neighboring stations, we present two experiments to evaluate and validate this method
187 by using IGS stations located in U.S. and Europe region. To ensure the accuracy and

188 consistency of DCB, we only select IGS stations with pseudorange measurements of
189 P1 code, and whose receiver DCBs have been published by CODE.

190 Figure 1 presents the location and distribution of the selected IGS stations in two
191 regions. Table 1 presents the information of the geographical location, distance to
192 reference station in each region and receiver types of all stations. Based on the
193 RINEX data of GOLD station in Region I and PTBB station in Region II during the
194 period of 2003-2013, two separate optimal ionospheric shell height models for each
195 region are established by the aforementioned method. Then the model are applied to
196 DCB estimation in 2014 for all the other stations in each region. Note that reference
197 GOLD and PTBB stations are marked with black triangle in the figure. The other
198 neighboring stations are located in different orientations of GOLD and PTBB with
199 different distances, which range from 136 to 1159 km for region I and range from
200 190.82 to 1712.27 km for region II. In the table, the receiver type is corresponding to
201 2003~2014 for GOLD and PTBB, and 2014 for the other stations. In region I, the
202 receiver type of GOLD has been changed once in September 2011. The five selected
203 stations used four receiver types in 2014; TABV and PIE1 had the same receiver type.
204 In region II, there are nine receiver types for the sixteen stations. The receiver type of
205 PTBB has changed twice in 2006.

206



207

208 **Fig.1** Geographical location of the selected IGS stations in U.S. region (Region I) and

209 Europe region (Region II). The black triangle in each plot is the reference station.

210

211

212 **Table 1** Information for the stations

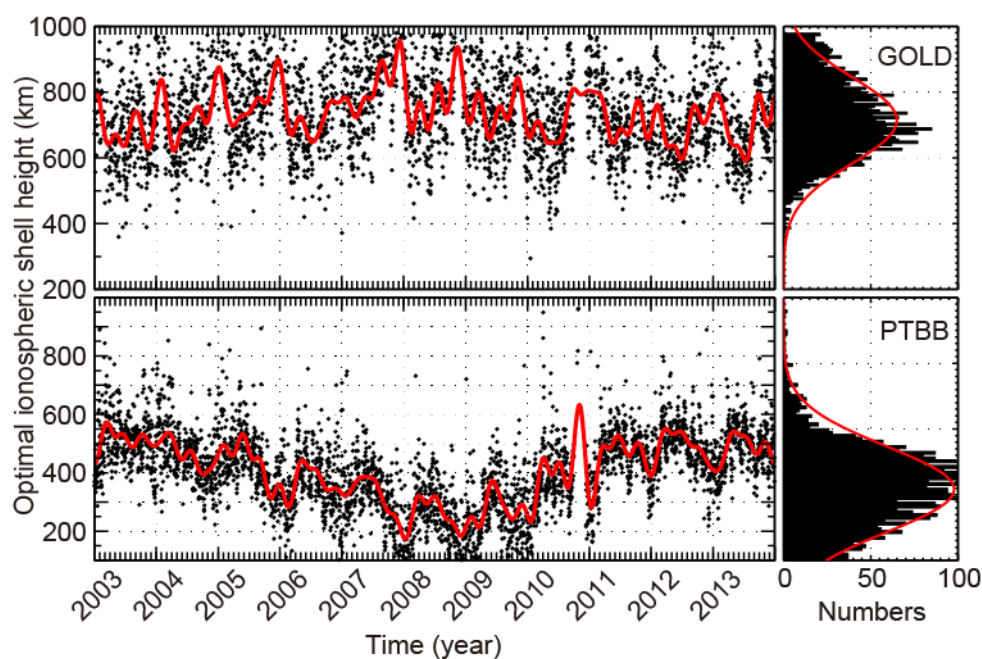
Name	Latitude (deg)	Longitude (deg)	Distance to GOLD or PTBB (km)	Receiver type and service date
GOLD	35.42	-116.89	0	ASHTECH Z-XII3 ~ 2011-09-14
TABV	34.38	-117.68	136.67	JPS EGGDT 2011-09-19 ~
				JAVAD TRE_G3TH DELTA

QUIN	39.97	-120.94	619.55	ASHTECH UZ-12
PIE1	34.30	-108.12	810.51	JAVAD TRE_G3TH DELTA
AMC2	38.80	-104.52	1159.09	ASHTECH Z-XII3T
				SEPT POLARX2 2006-07-25~
PTBB	52.15	10.30	0	2006-11-13
				ASHTECH Z-XII3T else
POTS	52.38	13.07	190.82	JAVAD TRE_G3TH DELTA
WSRT	52.91	6.60	264.92	AOA SNR-12 ACT
WTZA	49.14	12.88	381.28	ASHTECH Z-XII3T
WTZS	49.14	12.88	381.28	SEPT POLARX2
WTZZ	49.14	12.88	381.28	JAVAD TRE_G3TH DELTA
GOPE	49.91	14.79	401.51	TPS NETG3
BRUX	50.80	4.36	439.03	SEPT POLARX4TR
ONSA	57.40	11.93	593.72	JPS E_GGD
ZIMJ	46.88	7.47	620.79	JAVAD TRE_G3TH DELTA
SPT0	57.72	12.89	641.78	JAVAD TRE_G3TH DELTA
OPMT	48.84	2.33	674.24	ASHTECH Z-XII3T
HERS	50.87	0.34	705.38	SEPT POLARX3ETR
IENG	45.02	7.64	816.64	ASHTECH Z-XII3T
VILL	40.44	-3.95	1696.62	SEPT POLARX4
MADR	40.43	-4.25	1712.27	JAVAD TRE_G3TH DELTA

213

214 Figure 2 presents the estimated daily optimal ionospheric shell height of GOLD
215 and PTBB during the period from 2003 to 2013. The left panel shows the variation of
216 the daily optimal ionospheric shell height and the fitting result by (6). From the
217 overall trend, the variations of daily optimal ionospheric shell height for both two

218 stations appear wave-like oscillation during the 11 years period. In the right panel, the
 219 statistical result are fitted by a normal distribution. The mean and the standard
 220 deviation (STD) of the normal distribution are 714.3 and 185.4 km for GOLD,
 221 respectively. The mean and STD value for PTBB is 416.4 and 184.1 km, respectively.
 222 At the end of 2010, a gap appears, for the DCB provided by CODE is simultaneously
 223 anomalous (Zhao and Zhou, 2018), and the data during this period are abandoned.
 224

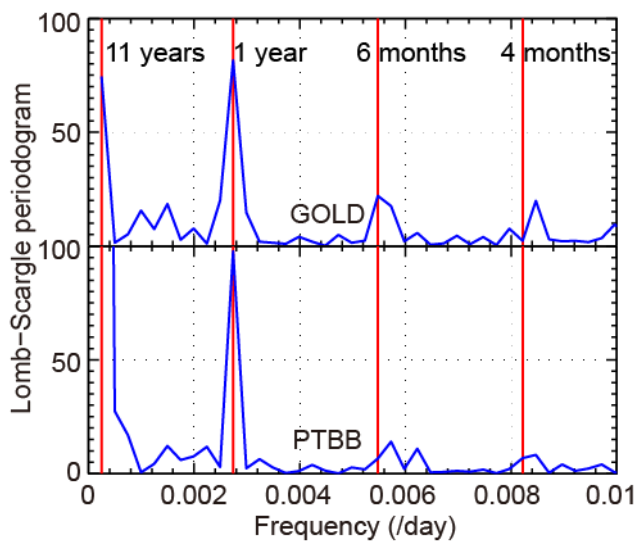


225
 226 **Fig.2** Variation of the daily optimal ionospheric shell height (black) and the fitting
 227 result (red)

228
 229 Figure 3 presents the amplitude spectra of the daily optimal ionospheric shell
 230 height of two reference stations estimated by the Lomb-Scargle analysis (Lomb, 1976;
 231 Scargle, 1982). As can be found in Figure 3, the peaks correspond to 11-year, 1-year,
 232 6-month and 4-month cycles. The amplitudes of 11-year and 1-year cycles are more

233 evident than other periods in both two stations. Note that the frequencies above 0.01
 234 per day are discarded because of their small amplitudes. As mentioned earlier, 0.01
 235 per day is about the maximum frequency of (6). This result shows that the optimal
 236 ionospheric shell height of GOLD and PTBB is periodic, and the 40th-order of
 237 Fourier series is suitable for modelling its variation.

238



239

240 **Fig.3** Lomb-Scargle spectra of the daily optimal ionospheric shell height

241

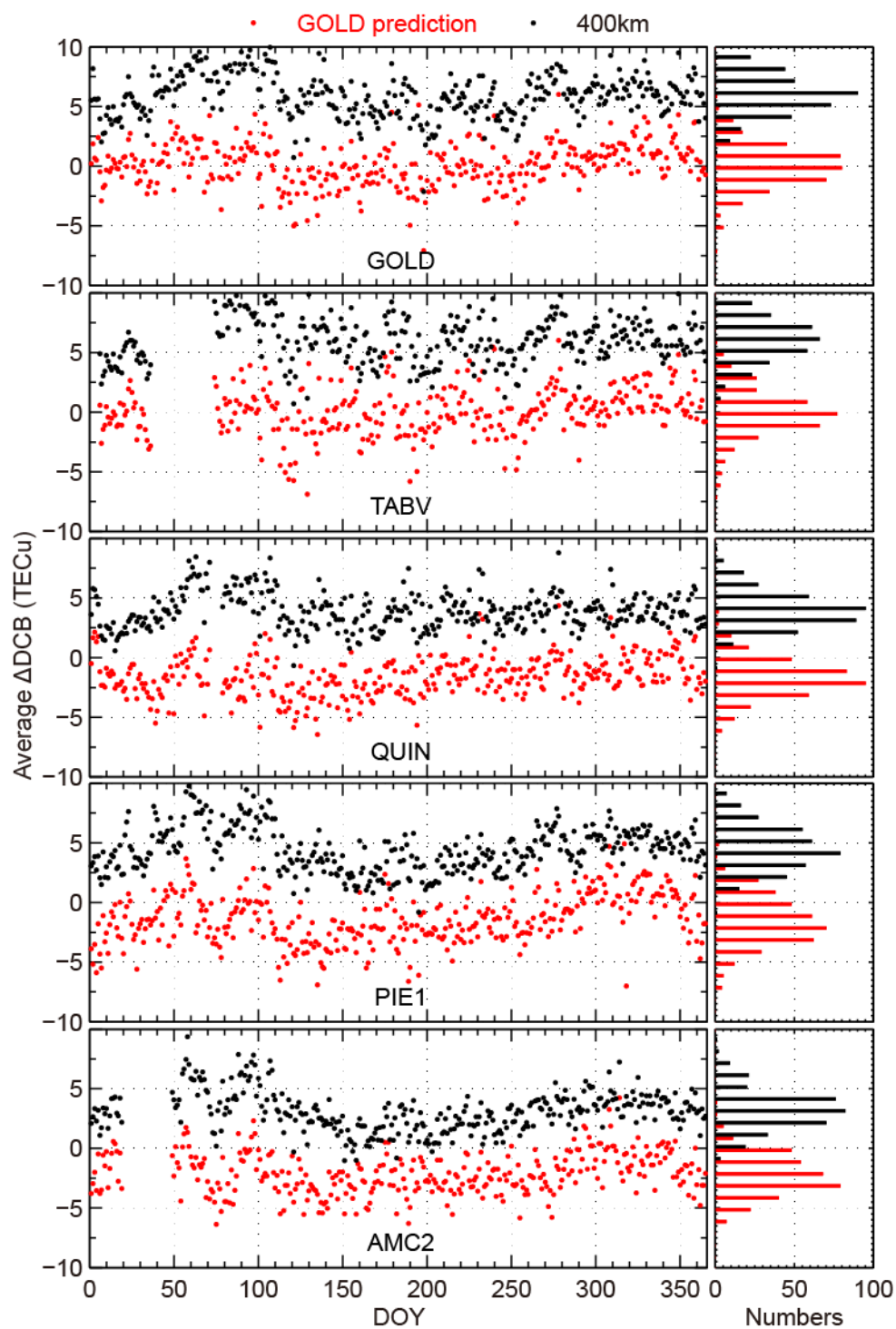
242 We establish two optimal ionospheric shell height models for each region by the
 243 40th-order of Fourier series based on the 11-year data of GOLD and PTBB. To
 244 investigate the availability zone of the optimal ionospheric shell height model, we
 245 apply the model to the stations of each region as shown in Figure 1 and Table 1. Based
 246 on the predicted daily optimal ionospheric shell heights in 2014 calculated by the
 247 model of GOLD and PTBB, the DCBs in all stations of each region are estimated in

248 the form of single station by the polynomial model mentioned earlier. The difference
249 of DCBs in all station in each region calculated by the optimal ionospheric shell
250 height model from each reference station and DCBs provided by CODE is then
251 compared to the difference of DCBs calculated by fixed ionospheric shell height (400
252 km) and DCBs released by CODE.

253 The results of this comparison are shown in Figure 4. The panels for the stations
254 are arranged by their distances to reference station, this is also applied to the
255 following table; from the top panels to the bottom panels, the distance of the
256 corresponding station to the reference station gradually increases. The left and right
257 panels show the daily differences and the histograms of the statistical results in 2014,
258 respectively. For all of the stations, the daily average differences of DCBs calculated
259 by the optimal ionospheric shell height model are reduced compared to the fixed
260 ionospheric shell height. For GOLD and TABV, the reductions are appropriate, the
261 daily average Δ DCBs around zero have the most days. For the other stations, the
262 reductions are so much that most of the average Δ DCBs are negative. This result
263 shows the improvement of the model seems to be related with the distance to GOLD.
264 Data gap on the figure correspond to days when data from that station are not
265 available. Figure 5 is the same format as Figure 4, which presents the results of
266 Region II. By comparing to the results of fixed ionospheric height, Figure 5 also
267 indicates that the Δ DCB calculated by using optimal ionospheric shell heights of
268 PTBB prediction is statistically less than that calculated by using fixed ionospheric

269 shell height. Both Figure 4 and Figure 5 present that the accuracy of DCB estimation
270 can be improved by using optimal ionospheric heights from reference station.

271



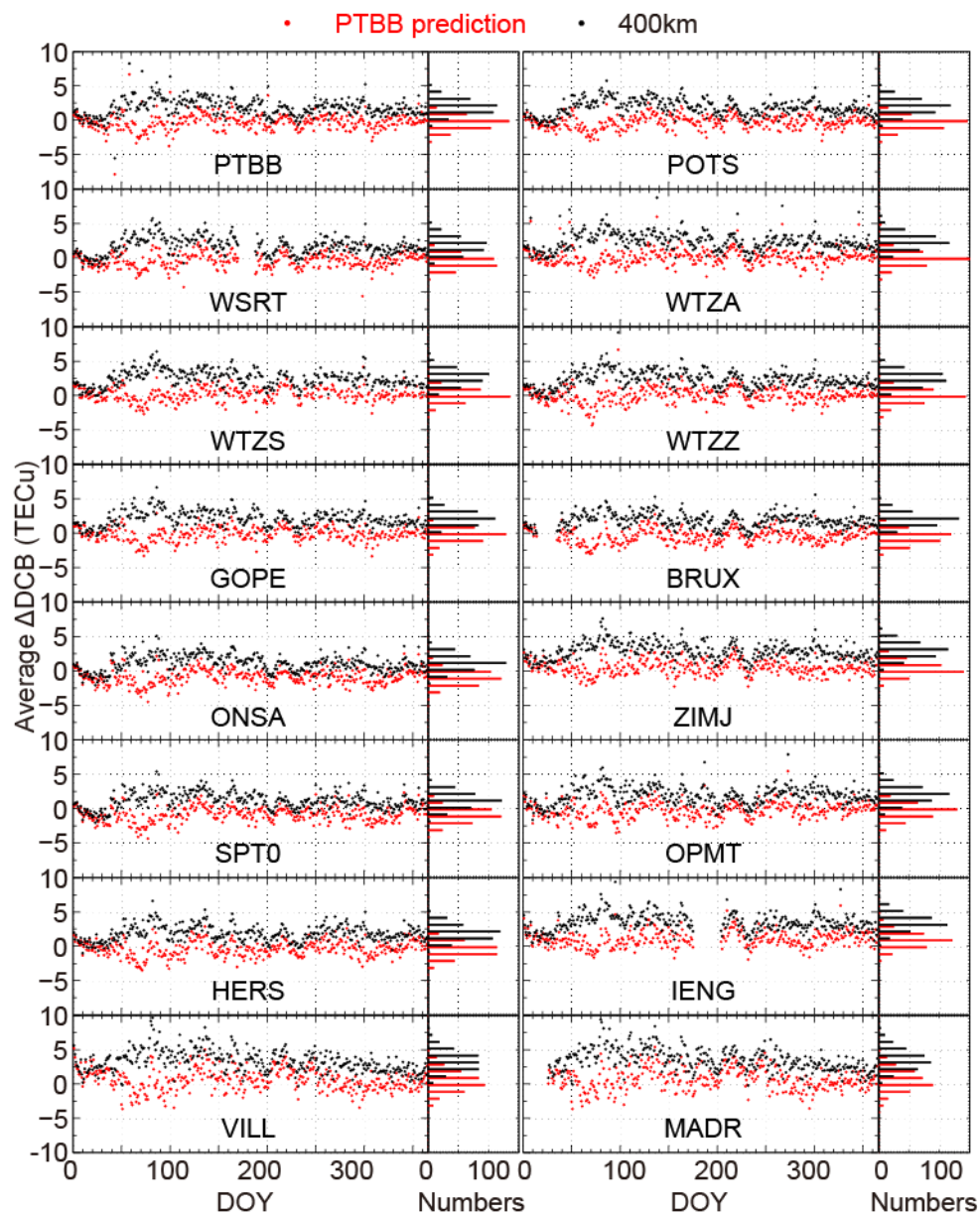
272

273 **Fig.4** Comparisons of the average Δ DCB calculated by the predicted optimal

274 ionospheric shell heights (red dots) and by the fixed ionospheric shell height (black
275 dots) in 2014 for stations in Region I.

276

277



278

279 **Fig.5** Comparisons of the average Δ DCB calculated by the predicted optimal
280 ionospheric shell heights (red dots) and by the fixed ionospheric shell height (black

281 dots) in 2014 for stations in Region II.

282

283 Table 2 presents the quantitative statistical results of average Δ DCB in 2014. For
284 all the stations in each region, the mean values and the root mean squares (RMS) by
285 the optimal ionospheric shell height model are smaller than by the fixed ionospheric
286 height. For Region I, the improvements of TABV are the most significant. Their mean
287 values are reduced to 0.12 and 0.08 TECu, respectively; the root mean squares are
288 reduced by 4.43 and 4.33 TECu, respectively. For Region II, the improvement for
289 DCB estimation are the most obvious for WTZZ, with mean value of Δ DCB decreases
290 from 2.34 to 0.02. We could note that TABV and WTZZ station are quite close to the
291 reference stations in each region.

292

293 **Table 2** Statistical results of mean (Δ DCB) in 2014

Station	Average Δ DCB (TECu)		Average Δ DCB (TECu)	
	Optimal Ionospheric Height		Fixed Ionospheric Height	
	Mean	RMS	Mean	RMS
GOLD	0.12	1.82	5.96	6.25
TABV	0.08	2.04	6.06	6.37
QUIN	-1.60	2.31	3.91	4.19
PIE1	-1.38	2.50	4.46	4.84
AMC2	-2.12	2.75	3.09	3.53
PTBB	-0.28	1.23	1.82	2.26
POTS	-0.27	1.00	1.84	2.18

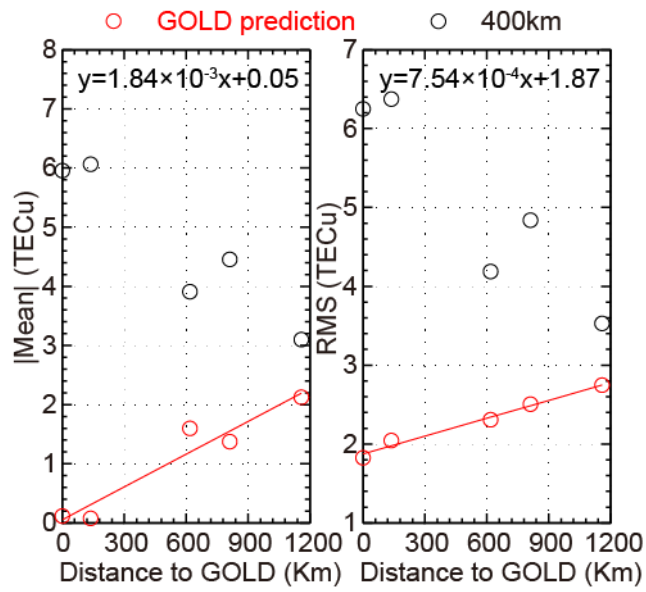
WSRT	-0.41	1.14	1.65	2.10
WTZA	0.09	1.20	2.38	2.73
WTZS	0.14	0.99	2.48	2.76
WTZZ	0.02	1.14	2.34	2.65
GOPE	-0.17	1.00	2.12	2.41
BRUX	-0.42	1.12	1.86	2.13
ONSA	-0.88	1.40	1.10	1.63
ZIMJ	0.48	1.17	2.87	3.13
SPT0	-0.84	1.40	1.14	1.67
OPMT	-0.29	1.21	1.93	2.35
HERS	-0.37	1.19	1.84	2.19
IENG	1.05	1.57	3.44	3.69
VILL	0.59	1.67	3.30	3.66
MADR	0.66	1.71	3.50	3.86

294

295 Figure 6 and Figure 7 present the relation between the statistical results of
296 average Δ DCB and the distance to reference stations in each region. The left and the
297 right panels in each figure show the relation of the absolute mean value and the root
298 mean square with the distance to GOLD and PTBB, respectively. For all of the
299 stations, the optimal ionospheric shell height model improves the accuracies of DCB
300 estimation compared to the fixed ionospheric shell height in a statistical sense; both of
301 the absolute mean values and the root mean squares become smaller. For the optimal
302 ionospheric shell height model, the absolute mean values present a positive
303 correlation with the distance to reference station GOLD and PTBB in each region, as

304 well as the root mean squares. By using the linear regression, for Region I, the
305 absolute mean value increases at a rate of about 1.84 TECu per 1000 km and start at
306 about 0.05 TECu. The RMS value increases at a rate of about 0.75 TECu per 1000 km
307 and starts at about 1.87 TECu. According to the fitting results, the absolute mean
308 value and the RMS less than 1 TECu and 2.25 TECu in the region around GOLD with
309 a radius of 500 km, and less than 2 TECu and 2.62 TECu for the region with a radius
310 of 1000 km. For Region II, the absolute mean value increases at a rate of about 0.30
311 TECu per 1000 km and start at about 0.25 TECu. The RMS value increases at a rate
312 of about 0.41 TECu per 1000 km and starts at about 1.01 TECu. According to the
313 fitting results, the absolute mean value and the RMS less than about 0.40 TECu and
314 1.21 TECu in the region around PTBB with a radius of 500 km, and less than about
315 0.55 TECu and 1.42 TECu for the region with a radius of 1000 km. For the two
316 regions, the RMSs presents stronger linear relation with distance comparing to the
317 means.

318



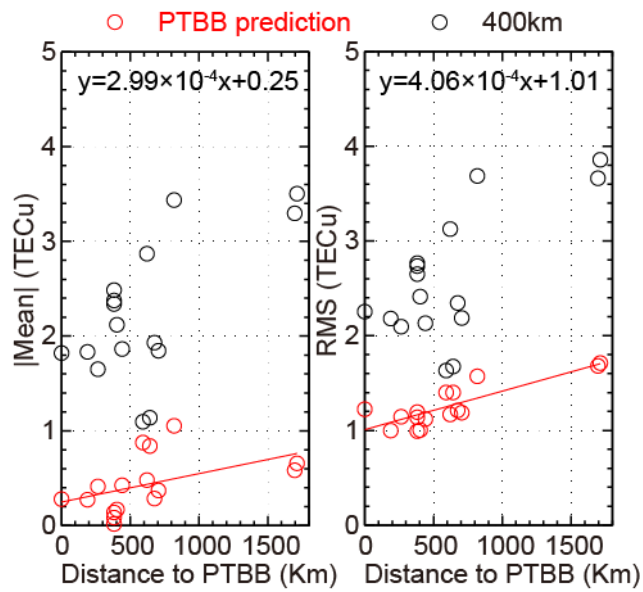
319

320 **Fig.6** Relation of the accuracy for DCB estimation with the distance to GOLD. The

321 red lines are the linear fitting results

322

323



324

325 **Fig.7** Relation of the accuracy for DCB estimation with the distance to PTBB. The

326 red lines are the linear fitting results

327

328

329 **Summary**

330 In this study, we investigate the implementation and validation of optimal ionospheric
331 shell height derived from IGS station to non-IGS station or isolated GNSS receiver.

332 We establish two optimal ionospheric shell height models by the 40th-order of Fourier
333 series based on the data of IGS station GOLD and PTBB in two separate regions

334 These two models are applied to the stations in each region, where the distance to
335 GOLD ranges from 136.67 to 1159.09 km and the distance to PTBB ranges from

336 190.82 to 1712.27 km. The main findings are summarized as follows:

337 1) The optimal ionospheric shell height model improves the accuracy of DCB
338 estimation comparing to the fixed shell height for all of the stations in a statistical
339 sense. This results indicate the feasibility of applying the optimal ionospheric shell
340 height derived from IGS station to other neighboring stations. The IGS station can
341 calculate and predict the daily optimal ionospheric shell height, and then release
342 this value to the nearby non-IGS stations or isolated GNSS receivers.

343 2) For other station in each region, the error of DCB by the optimal ionospheric shell
344 height increases linearly with the distance to the reference GOLD and PTBB
345 station. For the mean and the RMS of the daily average Δ DCBs, in region I, the
346 slopes are about 1.84 and 0.75 TECu per 1000 km; in region II, the slopes are
347 about 0.30 and 0.41 TECu per 1000 km. This results indicate the horizontal spatial
348 correlation of regional ionospheric electron density distribution. For different
349 region, the error at 0 km (i.e. the error for the reference station) is different, which

350 should be also considered.

351 As the requirement of this experiment, we just analyze two regions in
352 mid-latitude due to the insufficiency of long-term P1 data. We also ignore the
353 orientation of isolated GPS receivers to the reference station.

354

355 **Acknowledgments**

356 This study is based on data services provided by the IGS (International GNSS Service)
357 and CODE (the Center for Orbit Determination in Europe). This work is supported by
358 the National Natural Science Foundation of China (NSFC grant 41574146 and
359 41774162).

360

361 **Reference**

362 Birch, M. J., Hargreaves, J. K., Bailey, G. J.: On the use of an effective ionospheric
363 height in electron content measurement by GPS reception, *Radio Sci.*, 37, 1015,
364 doi: 10.1029/2000RS002601, 2002.

365 Brunini, C., Camilion, E., Azpilicueta, F.: Simulation study of the influence of the
366 ionospheric layer height in the thin layer ionospheric model, *J. Geod.*, 85,
367 637–645, doi: 10.1007/s00190-011-0470-2, 2011.

368 Clync, J. R., Coco, D. S., Coker, C. E.: A versatile GPS ionospheric monitor: high
369 latitude measurements of TEC and scintillation, in: *Proceedings of ION GPS-89,*
370 *the 2nd International Technical Meeting of the Satellite Division of The Institute*
371 *of Navigation, Colorado Springs, CO, 22–27 September 1989, 445-450, 1989.*

372 Horvath, I., Crozier, S.: Software developed for obtaining GPS-derived total electron
373 content values, *Radio Sci.*, 42, RS2002, doi: 10.1029/2006RS003452, 2007.

374 Huang, Z., Yuan, H.: Ionospheric single-station TEC short-term forecast using RBF
375 neural network, *Radio Sci.*, 49, 283–292, doi: 10.1002/2013RS005247, 2014.

376 Jiang, H., Wang, Z., An, J., Liu, J., Wang, N., Li, H.: Influence of spatial gradients on
377 ionospheric mapping using thin layer models, *GPS Solut.*, 22, 2, doi:
378 10.1007/s10291-017-0671-0, 2018.

379 Klobuchar, A.: Ionospheric time-delay algorithm for single-frequency GPS users,
380 *IEEE Trans. Aerosp. Electron. Syst.*, AES-23, 325–331, 1987.

381 Komjathy, A.: Global Ionospheric Total Electron Content Mapping Using the Global
382 Positioning System, Ph.D. thesis, Department of Geodesy and Geomatics
383 Engineering Technical Report NO. 188, University of New Brunswick,
384 Fredericton, New Brunswick, Canada, 248 pp., 1997.

385 Lanyi, G. E., Roth, T.: A comparison of mapped and measured total ionospheric
386 electron content using Global Positioning System and beacon satellite
387 observations, *Radio Sci.*, 23, 483–492, doi: 10.1029/RS023i004p00483, 1988.

388 Li, M., Yuan, Y., Zhang, B., Wang, N., Li, Z., Liu, X., Zhang, X.: Determination of
389 the optimized single-layer ionospheric height for electron content measurements
390 over China, *Journal of Geodesy*, 92, 169–183, doi: 10.1007/s00190-017-1054-6,
391 2018.

392 Lomb, N. R.: Least-squares frequency analysis of unequally spaced data,
393 *Astrophysics and space science*, 39, 447–462, doi: 10.1007/BF00648343, 1976.

394 Lu, W., Ma, G., Wang, X., Wan, Q., Li, J.: Evaluation of ionospheric height
395 assumption for single station GPS-TEC derivation, *Advances in Space Research*,
396 60, 286-294, doi: 10.1016/j.asr.2017.01.019, 2017.

397 Mannucci, A. J., Wilson, B. D., Yuan, D. N., Ho, C. H., Lindqwister, U. J., Runge, T.
398 F.: A global mapping technique for GPS-derived ionospheric total electron
399 content measurements, *Radio Sci.* 33, 565–583, doi: 10.1029/97RS02707, 1998.

400 Nava, B., Radicella, S. M., Leitinger, R., Coisson, P.: Use of total electron content
401 data to analyze ionosphere electron density gradients, *Adv. Space Res.*, 39,
402 1292–1297, doi: 10.1016/j.asr.2007.01.041, 2007.

403 Rideout, W., Coster, A.: Automated GPS processing for global total electron content
404 data, *GPS Solut.*, 10, 219–228, doi: 10.1007/S10291-006-0029-5, 2006.

405 Sardón, E., Rius, A., Zarraoa, N.: Estimation of the transmitter and receiver
406 differential biases and the ionospheric total electron content from global
407 positioning system observations, *Radio Science*, 29, 577–586, doi:
408 10.1029/94RS00449, 1994.

409 Scargle, J. D.: Studies in astronomical time series analysis. II-Statistical aspects of
410 spectral analysis of unevenly spaced data, *The Astrophysical Journal*, 263,
411 835-853, doi: 10.1086/160554, 1982.

412 Schaer, S.: Mapping and predicting the earth's ionosphere using the global positioning
413 system, Ph.D. thesis, Astronomical Institute, University of Bern, Bern,
414 Switzerland, 196 pp., 1999.

415 Smith, D. A., Araujo-Pradere, E. A., Minter, C., Fuller-Rowell, T.: A comprehensive
416 evaluation of the errors inherent in the use of a two-dimensional shell for

417 modeling the ionosphere, *Radio Sci.*, 43, RS6008, doi: 10.1029/2007RS003769,
418 2008.

419 Sovers, O. J., Fenslow, J. L.: Observation model and parameter partials for the JPL
420 VLBI parameter estimation software MASTERFIT-1987, JPL Publication,
421 California, , 68 pp, 1987.

422 Wang, X. L., Wan, Q. T., Ma, G. Y., Li, J. H., Fan, J. T.: The influence of ionospheric
423 thin shell height on TEC retrieval from GPS observation, *Res. Astron.*
424 *Astrophys.*, 16, 116, doi: 10.1088/1674-4527/16/7/116, 2016.

425 Warnant, R.: Reliability of the TEC computed using GPS measurements—the
426 problem of hardware biases, *Acta Geodaetica et Geophysica Hungarica*, 32,
427 451–459, doi: 10.1007/BF03325514, 1997.

428 Wild, U.: Ionosphere and satellite systems: permanent GPS tracking data for
429 modelling and monitoring, Ph.D. thesis, Astronomical Institute, University of
430 Bern, Bern, Switzerland, 155 pp., 1994.

431 Zhao, J., Zhou, C.: On the Optimal Height of Ionospheric Shell for Single-Site TEC
432 Estimation, *GPS Solut.*, 22, 48, doi: 10.1007/s10291-018-0715-0, 2018.

433 Zus, F., Deng, Z., Heise, S., Wickert, J.: Ionospheric mapping functions based on
434 electron density fields, *GPS Solut.*, 21, 873-885, doi:
435 10.1007/s10291-016-0574-5, 2017.

436